ResearchGate

See discussions, stats, and author profiles for this publication at: https://www.researchgate.net/publication/379336497

Graph theoretical analysis, pharmacoinformatics and molecular docking investigation of Chalcone-Schiff base hybrids as Cyclin-Dependent kinase inhibitors

Article *in* Research in Pharmacy · March 2024

DOI: 10.25081/rip.2024.v14.8801

CITATIONS
0

READS
53

6 authors, including:



Senthil Kumar Raju
Swamy Vivekanandha College of Pharmacy Elayampalayam Tiruchengode
193 PUBLICATIONS **2,745** CITATIONS
SEE PROFILE



Praveen Sekar
Swamy Vivekanandha College of Pharmacy, Tiruchengode, Namakkal, Tamilnadu, In…
38 PUBLICATIONS **79** CITATIONS
SEE PROFILE

Yogadharshini Nagalingam
8 PUBLICATIONS **3** CITATIONS
SEE PROFILE

Naveena Sundhararajan
Swamy Vivekanandha College Of Pharmacy Tiruchengode.
7 PUBLICATIONS **3** CITATIONS
SEE PROFILE

All content following this page was uploaded by Senthil Kumar Raju on 28 March 2024.

The user has requested enhancement of the downloaded file.

Research in Pharmacy 2024, 14: 1-15
doi: 10.25081/rip.2024.v14.8801
https://updatepublishing.com/journal/index.php/rip

Research Article



ISSN: 2231-539X

Graph theoretical analysis, pharmacoinformatics and molecular docking investigation of Chalcone-Schiff base hybrids as Cyclin-Dependent kinase inhibitors

Praveen Sekar, Sathishkumar Arivanantham, Pavithra Jaishanker, Naveena Sundhararajan, Yogadharshini Nagalingam, Senthil Kumar Raju*

Department of Pharmaceutical Chemistry, Swamy Vivekanandha College of Pharmacy, Tiruchengode, Namakkal-637 205, Tamil Nadu, India

ABSTRACT

One of the promising classes of compounds in medicinal chemistry and drug design is those with azomethine linkages. The Chalcone-Schiff base hybrids contain this linkage and some heteroatoms, which are versatile molecules, play a vital role in drug discovery and development with enormous therapeutic applications. In this view, the present work deals with the investigation of the *in silico* biological potential of the Chalcone-Schiff base hybrids based on the network pharmacology approach. From the results obtained from network pharmacology, the Cyclin-dependent kinase (CDK) isoforms were identified as the potential targets and the CDK inhibitory activity of the compounds was investigated using molecular docking studies. The *in silico* pharmacokinetic, metabolic and theoretical studies at DFT level were performed. Molecular docking studies revealed that the compounds have better CDK inhibitory potential with better binding affinity and interaction profile. Among the tested compounds, (Z)-2-((4,6-diphenyl-5,6-dihydro-4H-1,3-thiazin-2-yl)imino)-2,3-dihydro-1H-inden-1-one was found to be the most active compound than the standards, palbociclib and dinaciclib against the CDK isoforms (CDK1, CDK2 and CDK4) with the binding energies of -9.9, -10.3 and -10 Kcal/Mol, respectively. Also, this compound exhibited better pharmacokinetic and metabolic properties along with better solubility. The theoretical studies at the DFT level also indicate that the compound has better metabolic stability and the electron transfer from HOMO to LUMO was observed. Thus, the tested Chalcone-Schiff base hybrids can be used effectively for the inhibition of CDK isoforms.

Received: January 23, 2024
Revised: March 06, 2024
Accepted: March 07, 2024
Published: March 18, 2024

***Corresponding author:**
Senthil Kumar Raju
E-mail: thrisen@gmail.com

KEYWORDS: Schiff bases, Chalcone-based Schiff bases, Network Pharmacology, Enrichment analysis, Molecular docking, Theoretical studies

INTRODUCTION

Heterocyclic compounds are aromatic and/or cyclic molecules that have multiple heteroatoms, such as oxygen, sulphur, nitrogen and so on, arranged in rings. Despite the importance of heterocyclic compounds in medicine, there is still much to learn about them (Abdullah *et al.*, 2021). Medicinal chemistry is highly interested in fused heterocyclic compounds, which usually consist of five or six members, because of their diverse pharmacological and therapeutic implications. The Schiff bases, which are made by condensation of an aldehyde/ketone and amines, were one of the many heterocyclic compounds and derivatives that attracted the interest of organic chemists. Hugo Schiff discovered the Schiff bases in 1864. The functional group azomethine (C=N), commonly referred to as imines is present in these Schiff bases (Sekar *et al.*, 2023b). Chalcone Schiff base hybrids are important organic compounds that have recently attracted considerable interest for various biological applications. On the other hand, Chalcones or 1,3-diaryl-2-propen-1-ones, the precursor of flavonoids and isoflavonoids, consisted of α,β-unsaturated carbonyl system between two aromatic rings, which was found to be exhibiting various biological applications including anticancer, antimicrobial, anti-inflammatory, antioxidant, antidiabetic, antitubercular and antimalarial properties (Ejaz *et al.*, 2017; Sekar *et al.*, 2023a). Previously, various Chalcone Schiff base hybrids like chalcone sulphonamide hybrids (Ejaz *et al.*, 2017), tacrine-isatin Schiff base derivatives (Riazimontazer *et al.*, 2019),

Copyright: © The authors. This article is open access and licensed under the terms of the Creative Commons Attribution License (http://creativecommons.org/licenses/by/4.0/) which permits unrestricted, use, distribution and reproduction in any medium, or format for any purpose, even commercially provided the work is properly cited. Attribution — You must give appropriate credit, provide a link to the license, and indicate if changes were made.

semicarbazone and thiosemicarbazone 3-phenylquinazoline-2,4(1H,3H)-dione active Schiff bases (Muleta & Desalegn, 2022; Soman & Jain, 2022), ferrocene Chalcone-based Schiff bases (Liu *et al.*, 2018), 1,2,4-oxadiazole-chalcone/oxime hybrids Schiff base hybrids (Ibrahim *et al.*, 2021), hydrazinecarbothiamide and hydrazine-carboxamide Schiff base derivatives (Siddiqui *et al.*, 2019) and deoxybenzoin Chalcone-based Schiff base hybrids (Luo *et al.*, 2012) with anticancer (Liu *et al.*, 2018), antimicrobial (Aiwonegbe & Usifoh, 2021), antioxidant (Muleta & Desalegn, 2022), antidiabetic (Fandaklı *et al.*, 2018), immunosuppressant (Luo *et al.*, 2012) and tyrosine inhibitors (Radhakrishnan *et al.*, 2016), were reported.

Cyclin-dependent kinases (CDKs) are serine/threonine protein kinases whose activity depends on binding and activation by cyclin partners (Vadivelu *et al.*, 2014). Cyclins and cyclin-dependent kinases (CDKs) are two important types of molecules involved in cell cycle modulation in mammalian cells. The family of CDK proteins consists of 13 members, including CDK1 to CDK13. They are responsible for the regulations of proliferation, as well as involved in the transcription process. Due to the significance of these factors in the regulation of cancer cell proliferation, it is suggested that the blockade of these molecules can be considered a potent anti-cancer therapeutic approach in breast cancer. The substantial enhancement of cancer cell proliferation by increased CDK activity suggests that CDK inhibitors could be a unique and viable therapeutic method for treating cancer (Izadi *et al.*, 2023). The primary activators of the cell cycle are CDKs (cyclin-dependent kinases), which phosphorylate essential substrates to accelerate DNA synthesis and mitosis. CDKs are activated by cyclin binding and are strictly controlled throughout both proteolysis and synthesis. The activity of CDK is negatively regulated by the binding of tiny inhibitor proteins known as CDK inhibitors (CKIs). Thus, normal cell cycle progression requires cooperation between cyclin, CDKs and CKIs (Susanti & Tjahjono, 2021).

Many studies were focussed on the synthesis of various Chalcone-Schiff base hybrids. However, many of the authors had focussed only on the synthesis and characterization of such derivatives. Hence, we attempted to evaluate their biological potential based on the network pharmacology approach. Continuously, the molecular docking studies against the predicted targets, theoretical studies and *in silico* studies were performed.

MATERIALS AND METHODS

Ligand Preparation

Based on the literature survey, the list of 26 compounds, which are already synthesized and not evaluated biologically (Sekar *et al.*, 2023b) were collected and sketched using ChemDraw Ultra 12.0 (http://www.cambridgesoft.com) and energy minimization and geometry correction was done by using the Avogadro software. The outputs of the structures were saved in smiles, mol file (.mol) and pdb (.pdb) formats which were used for further *in silico* studies.

Target Prediction by Network Pharmacology Approach

Initially, the targets for the designed compounds were predicted by using the Swiss target prediction on the SwissADME web server. The most prominent and highly active targets from the Swiss target prediction were chosen for further molecular docking studies.

Construction of Target Protein-Protein Interaction (PPI) Network

Protein targets were used for protein–protein interaction (PPI) analysis using the STRING 3.0 database (https://string-db.org/). A minimal interaction network was selected for additional Cytoscape investigation. Common genes linked with the disease targets were first identified for the PPI network using the Venn plot tool (https://bioinformatics.psb.ugent.be/webtools/Venn/) and the Swiss target prediction tool for the predicted targets.

Enrichment Analysis and KEGG Pathway

The gene enrichment analysis and KEGG pathway of the title compounds were obtained using the Shinygo 0.77 webserver (http://bioinformatics.sdstate.edu/go/) by employing the common genes obtained from the Venn plot. The top pathways were selected and the top most active target against the designed compounds was identified.

Network Visualization

The networks were constructed by utilizing the Cytoscape software. Moreover, some networks were directly exported from the *in situ* web-based platform like the STRING database. The predicted targets and network against Cyclin-dependent Kinase were obtained in simple hierarchical networks (Shannon *et al.*, 2003). Thus, based on the most prominent targets and common pathways obtained from the Swiss target prediction and Network pharmacology approach, the targets for the molecular docking studies were selected.

Protein Preparation

Crystal three-dimensional structures of Cyclin-dependent Kinase 1 (PDB ID: 6GU6) Cyclin-dependent Kinase 2 (PDB ID: 2R3I) and Cyclin-dependent Kinase 4 (PDB ID: 2W9Z) were downloaded from RCSB Protein Data Bank (http://rscb.org) in the.pdb format. The stereochemical properties of each target protein were assessed based on the information obtained from the PDB X-ray structure Validation Report for each PDB structure. The resolution and R-values showed the goodness of the protein model being used. The X-ray crystal structure with resolution values of 2.0 Å or less and R-values of 0.2 or less are considered acceptable. Proteins were energy minimized, water molecules and cocrystallized ligands were removed, polar hydrogen and Kollman charges were added. Finally, 3D structures of the target proteins were saved in.pdbqt format and used for docking studies.

Molecular Docking and Visualization

Molecular docking was performed using AutoDock 4.2 (http://autodock.scripps.edu/) with the Lamarckian genetic algorithm. The docking parameters selected were 20 docking runs and a population size of 150. The binding energy of the protein coordinate was evaluated by a three-dimensional grid box of 90x90x90 (Number of grid points in xyz) created with a spacing of 0.375 Å (Morris *et al.*, 2009). Biovia Discovery Studio version 21.1.0 (https://www.3dsbiovia.com/) was used to visualize the docking results. The docking energies of the designed compounds were compared with the commercially available CDK inhibitors for the validation of results. The docking energy for a given protein-ligand pair comprised of the intermolecular interaction energies including internal steric energy, hydrogen bond interaction energy, Van der Waals force and Coulombic electrostatic energy of the compounds. The lowest binding energy of the protein-ligand complex has been considered to be the best.

Physicochemical Properties, Drug-likeness, Pharmacokinetic Parameters and Toxicity Prediction

The physicochemical properties, pharmacokinetic parameters, drug-likeness and toxicity studies of the listed compounds were predicted to determine the druggable nature of the compounds, also important in terms of reducing their side effects on the target organism. The physicochemical properties and drug-likeness properties were predicted using the SwissADME (http://www.swissadme.ch) web server. The ADMET properties of the query molecules were predicted by using pkCSM (https://biosig.lab.uq.edu.au/pkcsm/) and ProTox II (https://tox-new.charite.de/protox_II/) webservers. In addition, the LD_{50} values and toxicity classes of the compounds were predicted using ProTox-II, along with the organ toxicities was also predicted. Cardiotoxicity of these compounds was predicted by using the cardio ToxCSM webserver (https://biosig.lab.uq.edu.au/cardiotoxcsm/).

Theoretical Studies

On a personal computer, the full set of calculations was carried out at the DFT level using the Gaussian 09 W, GaussView 6.0, and ChemDraw Ultra 12.0 software. The density functional theory or DFT was used to perform the theoretical computations for the lead compound identified using molecular docking studies. The best structural parameters for the molecule were found using the B3LYP functional and the B3LYP/6-31G ++ (d, p) basis set. The potential energy surface at the 6-31 G ++ (d, p) level was studied. All the parameters were permitted to relax and the calculation converged to an optimized shape that corresponded to a true minimum (Ermiş, 2018; Datar *et al.*, 2024).

RESULTS AND DISCUSSION

CDKs are a class of serine/threonine kinases that play essential functions in controlling the advancement of the cell cycle. Cyclins stimulate these kinases to become active. The orderly course of the cell cycle is regulated by CDK/cyclin complexes. Recent research indicates that CDKs and cyclins actively regulate transcription, metabolic processes, epigenetic mechanisms and stem cell's ability to rejuvenate themselves (Ghafouri-Fard *et al.*, 2022). There are 13 members in the CDK protein family, ranging from CDK1 to CDK13. They are divided into members that control proliferation, such as CDK1, 2, 3, 4 and 6, members that are involved in transcription, such as CDK7, 8, 9, 11, 12 and 13. Given their significant influence over the regulation of the growth of cancer cells, it is proposed that blocking these molecules may represent a highly effective anti-cancer treatment strategy (Izadi *et al.*, 2023). Thus, an attempt was made to predict the biological potential of the previously described Chalcone-Schiff base hybrids based on the network pharmacology and other *in silico* studies. The structures of the selected compounds are given in Figures 1 and 2. The names, compound numbers and references of the compounds are given in Table 1.

Network Pharmacology

Initially, the targets responsible for the designed compounds were predicted utilizing the SWISS Target Prediction webserver, which revealed that the compounds were active against different types of cancers, especially against various types of CDKs, Cell cycle, Cyclin binding and Serine/Threonine protein kinases. Based on the targets obtained from the SWISS Target Prediction analysis, the genes responsible for CDKs were retrieved from GeneCards and OMIM databases. From the obtained list of genes, the 15 common genes were identified using the Venny database and given in Figure 3a.

Construction and Analysis of Protein-Protein Interaction

PPI network which contains 15 nodes and 55 edges was primitively constructed by the STRING database, in which nodes represent proteins and edges stand for protein-protein interactions, given in Figure 3b. The other parameter is the average node degree which values at 7.33 and the average local clustering coefficient of 0.73 corresponds to the number of targets that are connected to the network. To further visualize and analyze the protein-protein interactions, the retrieved PPI data were subsequently imported into Cytoscape 3.8.0 to construct a new PPI network, which also includes 15 nodes and 55 edges, given in Figure 3c. Subsequently, the Cytohubba plugin software was utilized for mining the targets suitable for molecular docking analysis. The top 10 calculations based on the degree were utilized on the Cytohubba plugin software and the top targets for which the compounds are active were identified. Based on this analysis, it merely showed that those candidate proteins are strongly related to each other in Epidermal Growth Factor Receptor (EGFR). Epidermal Growth Factor Receptor (EGFR) belongs to receptor tyrosine kinase (RTK) which is found in the plasma membrane, and it has a function to regulate cell growth. Each protein such as PIK3CA, MAPK1 and CASP3 was also found to be the most prominent targets and correlates with the targets obtained from enrichment analysis and STRING database. Even the Cyclin-dependent kinase

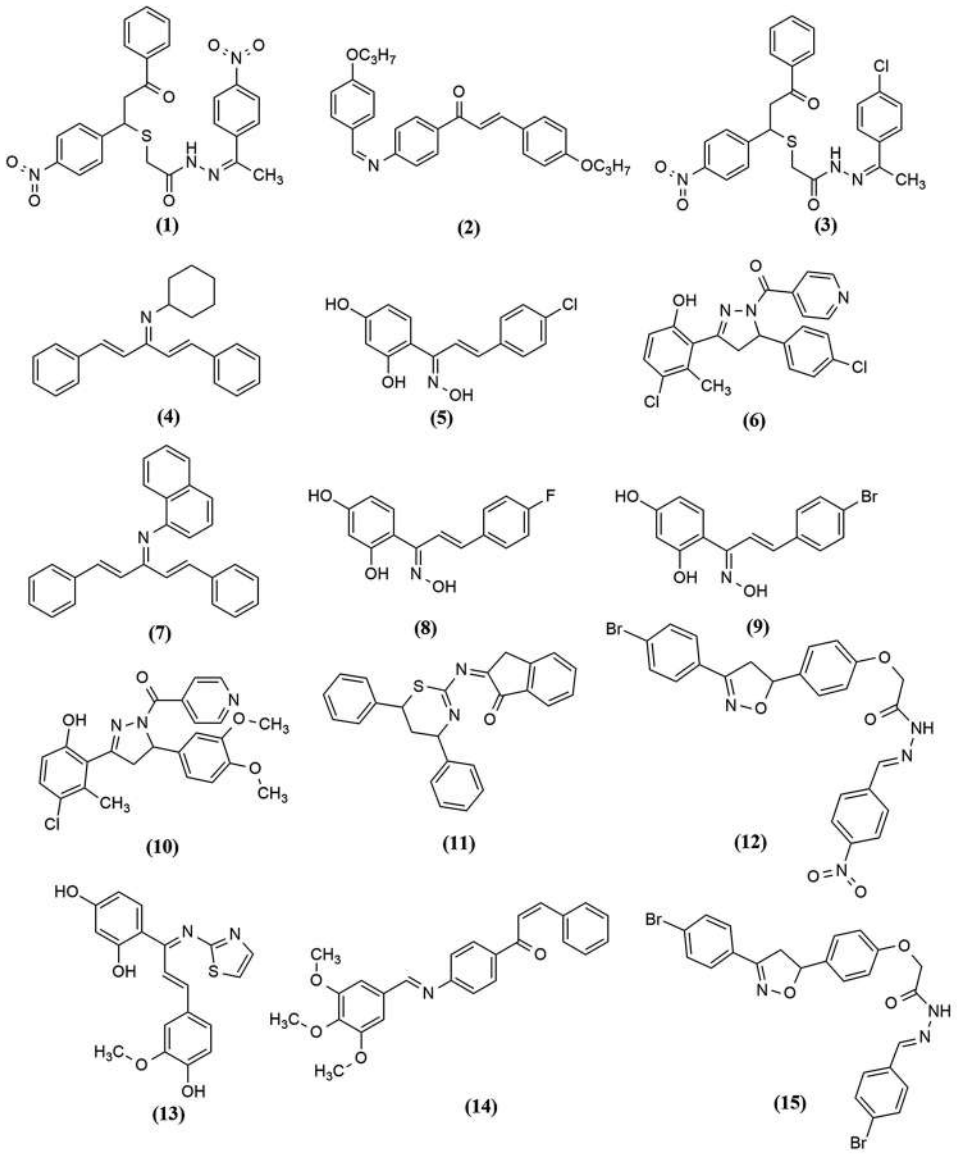

Figure 1: Structures of selected compounds (1-15)

inhibition has a lesser probability, based on our hypothesis; CDKs were chosen as prominent targets.

Enrichment Analysis

GO (Gene Ontology) and KEGG pathway enrichment analysis were used to explore the functions and enriched pathways of the putative CDK inhibitory genes of the designed compounds, analyzed using the ShinyGo 0.77 database. The GO analysis consists of biological processes (BP), cellular components (CC), and molecular functions (MF). The criteria include humans as the best matching species, FDR cutoff of 0.05 and top 10 pathways to show. The biological process represents the larger cellular or physiological role carried out by the gene, the cellular component represents the location in the cell where the gene product executes its function and the Molecular function represents the molecular activity of a gene. False Discovery Rate (FDR) measures the proportion of false discoveries among a set of hypothesis tests called significant. This quantity is typically estimated based on p-values or test statistics. In some scenarios, there is additional information available that may be used to more accurately estimate the FDR. An FDR <0.05 was used to indicate significant differences between GO terms and KEGG pathways (Shawky, 2019; Kawsar et al., 2020; Chen et al., 2021; Li et al., 2022;). A knowledge base for the systematic analysis of gene functions, KEGG (Kyoto Encyclopaedia of Genes and Genomes) connects genomic data with higher-level functional data. The GENES database, which is a compilation of gene catalogues for all fully sequenced genomes and some partially sequenced genomes with current annotation of gene functions, is where the genomic data is kept (Shawky, 2019).

The KEGG pathways were applied to explore the functions and signalling pathways of the identified CDK targets of designed compounds. There were numerous statistically significant

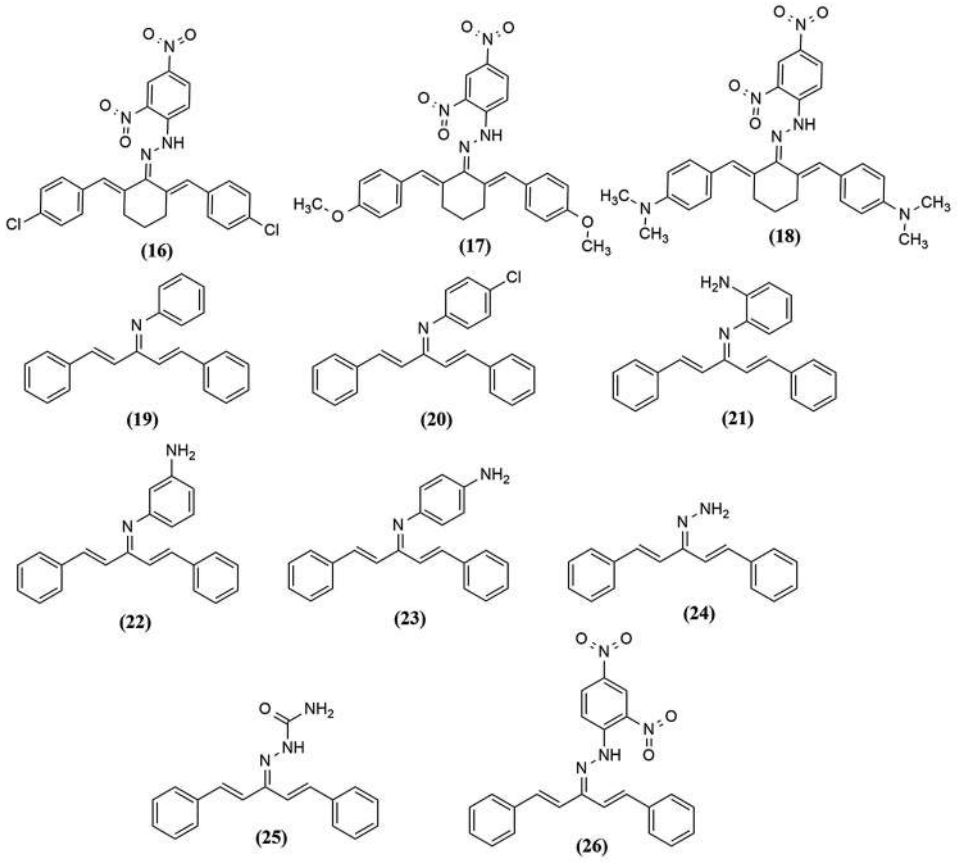

Figure 2: Structures of selected compounds (16-26)

Table 1: Compound numbers, names and references of the selected compounds

Compound No.	Compound Name	References
1	1-((2E,6E)-2,6-bis (4-chlorobenzylidene) cyclohexylidene)-2-(2,4-dinitrophenyl) hydrazine	Ahmed *et al.*, 2022
2	1-((2E,6E)-2,6-bis (4-methoxybenzylidene) cyclohexylidene)-2-(2,4-dinitrophenyl) hydrazine	Thakare & Mandlik, 2017
3	4,4'-((1E,1'E)-(2-(2-(2,4-dinitrophenyl) hydrazono) cyclohexane-1,3-diylidene) bis (methanylylidene)) bis (N, N-dimethylaniline)	Ahmed *et al.*, 2022
4	(Z)-2-((1-(4-nitrophenyl)-3-oxo-3-phenyl propyl) thio)-N'-(1-(4-nitrophenyl) ethylidene) acetohydrazide	Ajani *et al.*, 2021
5	(Z)-N'-(1-(4-chlorophenyl) ethylidene)-2-((1-(4-nitrophenyl)-3-oxo-3-phenylpropyl) thio) acetohydrazide	Dangwal & Semwal, 2016
6	(E)-1-(4-((Z)-(4-propoxybenzylidene) amino) phenyl)-3-(4-propoxyphenyl) prop-2-en-1-one	Thakare & Mandlik, 2017
7	(3-(3-chloro-6-hydroxy-2-methylphenyl)-5-(4-chlorophenyl)-4,5-dihydro-1H-pyrazol-1-yl) (pyridin-4-yl) methanone	Ajani *et al.*, 2021
8	N-((1E,4E)-1,5-diphenylpenta-1,4-dien-3-ylidene) aniline	Dangwal & Semwal, 2016
9	4-chloro-N-((1E,4E)-1,5-diphenylpenta-1,4-dien-3-ylidene) aniline	Dangwal & Semwal, 2016
10	N1-((1E,4E)-1,5-diphenylpenta-1,4-dien-3-ylidene) benzene-1,2-diamine	Thakare & Mandlik, 2021
11	N1-((1E,4E)-1,5-diphenylpenta-1,4-dien-3-ylidene) benzene-1,3-diamine	Rohini *et al.*, 2021
12	N1-((1E,4E)-1,5-diphenylpenta-1,4-dien-3-ylidene) benzene-1,4-diamine	Jamel *et al.*, 2017
13	N-((1E,4E)-1,5-diphenylpenta-1,4-dien-3-ylidene) naphthalen-1-amine	Vyas, 2018
14	N-((1E,4E)-1,5-diphenylpenta-1,4-dien-3-ylidene) cyclohexanamine	Vyas *et al.*, 2016
15	((1E,4E)-1,5-diphenylpenta-1,4-dien-3-ylidene) hydrazine	Jamel *et al.*, 2017
16	2-((1E,4E)-1,5-diphenylpenta-1,4-dien-3-ylidene) hydrazinecarboxamide	Badal *et al.*, 2020
17	1-(2,4-dinitrophenyl)-2-((1E,4E)-1,5-diphenylpenta-1,4-dien-3-ylidene) hydrazine	Badal *et al.*, 2020
18	(Z)-3-phenyl-1-(4-((E)-(3,4,5-trimethoxy benzylidene) amino) phenyl) prop-2-en-1-one	Badal *et al.*, 2020
19	(1E,2E)-3-(4-chlorophenyl)-1-(2,4-dihydroxyphenyl) prop-2-en-1-one oxime	Ajani *et al.*, 2021
20	(1E,2E)-1-(2,4-dihydroxyphenyl)-3-(4-fluorophenyl) prop-2-en-1-one oxime	Ajani *et al.*, 2021
21	(1E,2E)-3-(4-bromophenyl)-1-(2,4-dihydroxyphenyl) prop-2-en-1-one oxime	Ajani *et al.*, 2021
22	(3-(3-chloro-6-hydroxy-2-methylphenyl)-5-(3,4-dimethoxyphenyl)-4,5-dihydro-1H-pyrazol-1-yl)(pyridin-4-yl) methanone	Ajani *et al.*, 2021
23	(Z)-2-((4,6-diphenyl-5,6-dihydro-4H-1,3-thiazin-2-yl) imino)-2,3-dihydro-1H-inden-1-one	Ajani *et al.*, 2021
24	(E)-2-(4-(3-(4-bromophenyl)-4,5-dihydroisoxazol-5-yl) phenoxy)-N'-(4-nitrobenzylidene) acetohydrazide	Ajani *et al.*, 2021
25	(E)-N'-(4-bromobenzylidene)-2-(4-(3-(4-bromophenyl) -4,5-dihydroisoxazol-5-yl) phenoxy) acetohydrazide	Ajani *et al.*, 2021
26	4-((1E,2E)-3-(4-hydroxy-3-methoxy phenyl)-1-(thiazol-2-ylimino) allyl) benzene-1,3-diol	Ajani *et al.*, 2021

pathways, among them, the top 10 significant enrichment potential pathways based on KEGG, BP, CC and MF with the highest gene counts were presented in bar plot diagrams and the KEGG pathway is given in Figures 4 and 5, indicating that the designed compounds play an important role in the inhibition of CDK through multiple targets. Based on the obtained enrichment analysis results, it was proved that the designed compounds will be used for CDK inhibition. Cyclin-dependent protein serine/threonine kinase activity, Cyclin binding, Cell cycle, P53 signalling pathway, PI3K-Akt signalling pathway, Cyclin D2-CDK4 complex, Cyclin-dependent protein kinase holoenzyme complex, Cell cycle G1/S phase transition. G1/S transition of mitotic cell cycle and cell division are responsible for the CDK inhibitory activity, obtained by GO, Enrichment and KEGG pathway analysis. According to these results, most of the obtained pathways are related to CDK inhibition, i.e., related to the cell cycle, CDK and cyclin binding. Even though the CDK targets had the least probability on network analysis, based on the enrichment analysis and correlation of GO, KEGG and network, we had chosen the CDK isoforms as the query targets for the study. CDKs are a group of enzymes that play a crucial role in regulating the cell cycle. Abnormal activation of CDKs can lead to uncontrolled cell division, a hallmark of cancer. The implication here is that inhibiting CDK

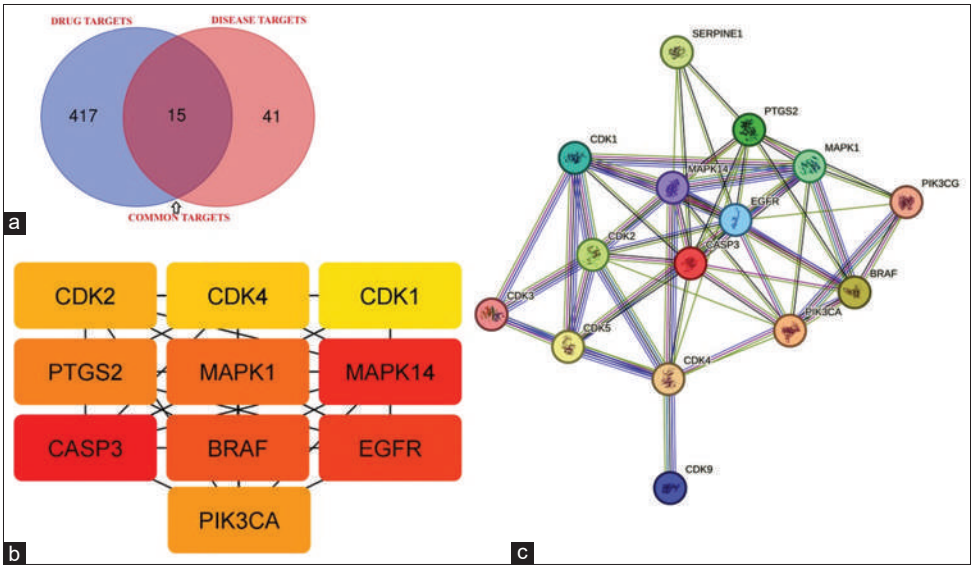

Figure 3: a) Venn diagram showing the common targets responsible for network construction, b) Network visualization using Cytoscape software, c) Protein - Protein Interaction Network obtained using STRINGv_11. 5 database

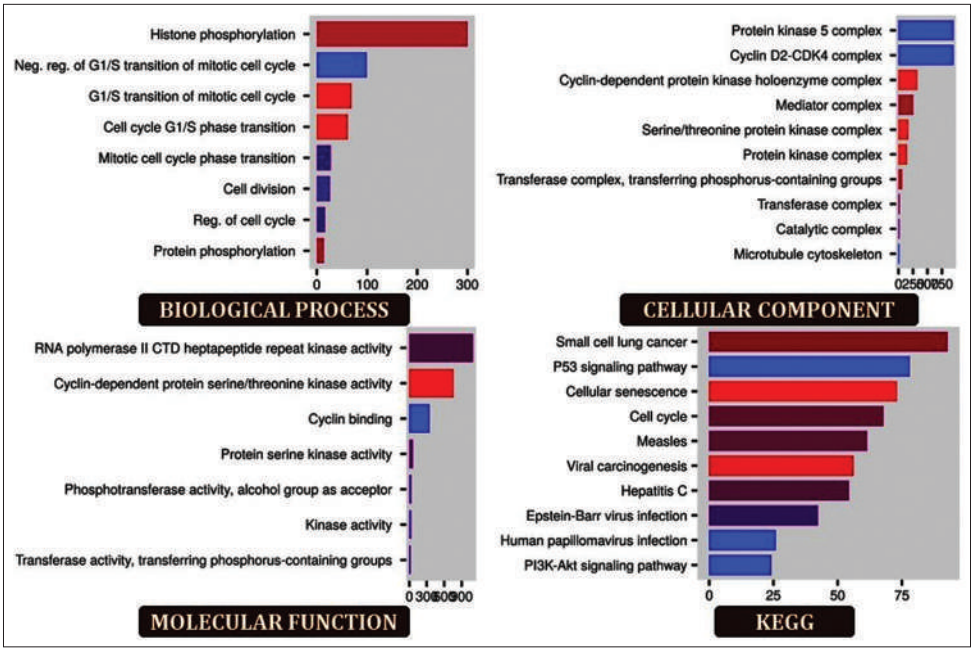

Figure 4: Top 10 Pathway Enrichment analysis

activity could be an effective strategy to slow down or stop the proliferation of cancer cells. CDK inhibitors are compounds designed to block the activity of these enzymes. The structure of CDK inhibitors is said to be related to anion transporter polypeptides (ATP). ATP is a molecule involved in cellular energy transfer. The statement suggests that CDK inhibitors compete with kinases (including CDKs) for binding to ATP. CDK inhibitors are characterized as having selective inhibition, meaning they specifically target CDKs without affecting other kinases excessively. Additionally, they are noted for low toxicity, indicating that they may have fewer adverse effects on normal, healthy cells. The selective nature of CDK inhibitors and their potential for low toxicity make them attractive as alternatives to traditional chemotherapies. Chemotherapies often target rapidly dividing cells, which can include both cancer and normal cells, leading to side effects. CDK inhibitors, by selectively targeting the abnormal cell cycle regulation in cancer cells, might offer a more targeted and less toxic therapeutic approach (Izadi *et al.*, 2023). Based on the above results, the CDK inhibitory potential of the designed compounds was further analysed through molecular docking studies.

Molecular Docking Studies

Based on the network pharmacology studies, three candidate target proteins, including CDK1 (PDB ID: 6GU6), CDK2 (PDB ID: 2R3I) and CDK4 (PDB ID: 2W9Z) were selected as the most appropriate targets and conducted molecular docking with the designed compounds using Autodock 4.2 software. Their resolved crystal structures were downloaded from the Protein Data Bank. Further, the proteins were validated by Ramachandran plot and the percentage residues present in the favourable region were calculated. The entire target proteins showed more than 90% of the favourable region indicating that all the target proteins are valid targets for drug screening. The molecular docking results of the designed compounds against the selected CDK targets revealed that compound 23 was found to have better binding energy and interaction profile against all three targets by showing Vander Waals interactions, conventional hydrogen bond interactions, carbon-hydrogen bond interactions, π-anion interactions, π-sulphur interactions, π-π T-stacked interactions, π-sigma interactions and π-alkyl interactions with various interacting amino acid residues including GLU 38, ILE 35, ARG 36, LEU 37, GLU 40, ILE

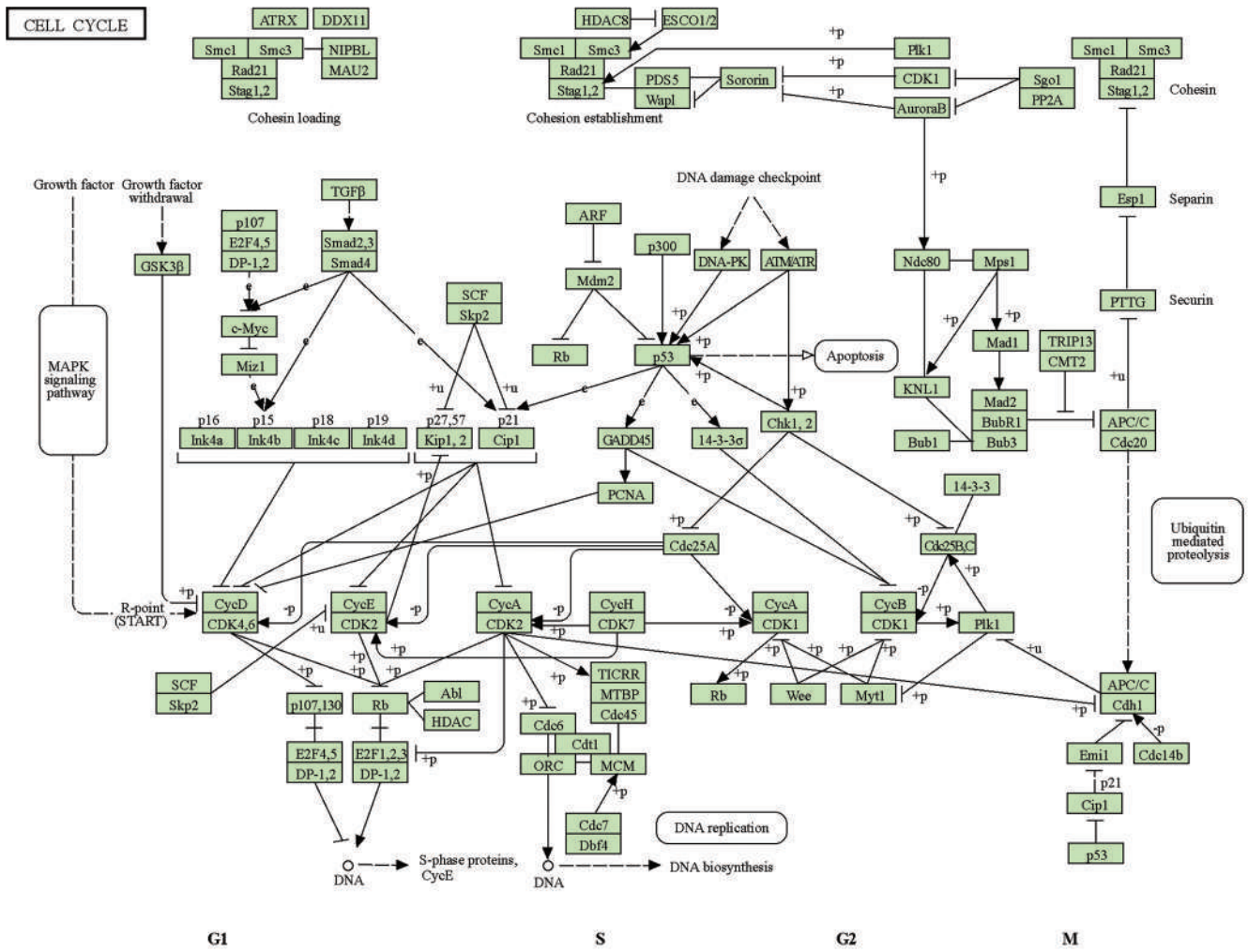

Figure 5: KEGG pathway for Cell cycle and CDK inhibition

49, SER 46, TYR 15, THR 14, GLY 154, ALA 152, PHE 153, ILE 155, THR 47, ALA 48, LYS 112, MET 113, VAL 109, GLU 141, LEU 142, VAL 145, LEU 152, TRP 150, ARG 200, PRO 204, PRO 204, PRO 130, YR 168, LYS 129, THR 165, GLN 131, LYS 88, TRP 167, GLU 195, MET 91, MET 196, SER 94, ARG 199, GLY 98, ALA 95, ASP 92 and ALA 201 respectively. In order to assess the degree of affinity that substances have with protein targets, the binding energy was often measured. According to common wisdom, binding energies of less than −4.25, −5.0 or −7.0 kcal/mol, respectively, suggest a certain, strong, or good level of binding activity between the ligand and the receptor. The potential for binding between the ligand and receptor is reflected in the binding energy. The more stable the conformation, the lower the binding energy and the higher the affinity of the ligand and receptor (Liu *et al.*, 2021). The results of docking binding energy in Table 2 revealed that these compounds could bind well to the active sites of protein targets as that of standard drugs. Among them, compound 23 was found to be the better compound against CDK inhibition with the binding energies of -9.9 kcal/mol against CDK1, -10.2 kcal/mol against CDK2 and -10.0 kcal/mol against CDK4, mirroring a good or even strong binding activity in the molecular docking than the standard anti-CDK drugs Palbociclib and Dinaciclib. The docking results of the designed compounds are given in Table 2 and the interaction images of a better compound are given in Figure 6.

Prediction of Physicochemical, Pharmacokinetic Properties and Drug Toxicity

The influence of a chemical's diverse physicochemical characteristics on the biomolecules it interacts with is related to the pharmacological or therapeutic effect. The pharmacokinetic behaviour of drug candidates is significantly influenced by several physicochemical factors. The compound's SMILES format was entered and their physical characteristics, including lipophilicity, water solubility, pharmacokinetic profile, drug-likeness and lead likeness, were examined. The number of rotatable bonds, the number of H-bond donors and acceptors, the fraction Csp3, the Topological Polar Surface Area (TPSA) and the lipophilicity were all determined using the SwissADME website. According to this tool, if the TPSA is <140 Å^2 and Log P (lipophilicity) < 5, the molecule will have apparent polarity, hence well absorbed by the GI tract when taken orally and prone to cross the BBB to enter the CNS (Pacey *et al.*, 2008). The TPSA and LogP values of the potent compound (compound 23) were about 67.09 Å^2 and 4.79, respectively, indicating that the compound had considerable permeability and absorption across the cellular plasma membrane. The fraction of sp3 carbon atoms (FCsp3) determines the carbon saturation of molecules and the FCsp3 ≥ 0.42 indicates the saturation and solubility profile (Kombo *et al.*, 2013), compound 23 with the FCsp3 value of 0.26 indicates that the compound has a unsaturation and lower solubility. A compound is regarded as a good candidate for oral administration if its molecular weight is less than 500 Dalton, its consensus log P value is less than or equal to 5, its number of rotatable double bonds is less than 10, its number of hydrogen bond donors is less than 5 and its total polar surface area is less than 140. The Lipinski (rule of five) describes the relationship between pharmacokinetic and physicochemical parameters whether the target compounds are likely to be bioactive and qualitatively assesses the possibility of these compounds becoming oral drug candidates. This allows researchers to distinguish between chemical substances that are drug-like and those that are not. MW ≤ 500; M log P ≤ 5; H-acc ≤ 10 and H-don ≤ 5 are all described by Lipinski's rule (Hassan *et al.*, 2023). Also, the potent compound exhibited a molecular weight of 396.5 (less than 500 Dalton), H-bond acceptors-03 (Less than 10), H-bond donors-01 (Less than 05), number of rotatable bonds-03 (Less than 10) and molar refractivity-123.88 (40 ≤ MR ≤ 140), these indicating the druggable nature of the compound. Based on this rule, the query compound fulfilled the needs and zero violations with a bioavailability score of 0.55 were observed against the Lipinski, Ghose, Veber and Egan filters, indicating that the potent compound (compound 23) reached the circulation system. The compound was also screened for PAINS alert and found to be non-toxic and metabolically stable with better lead likeness properties. The physicochemical and drug likeness properties of the selected compounds are given in Table 3 and RADAR diagrams of the compounds are given in Figure 7.

Table 2: Binding energies of compounds along with standards against the selected targets

Compound No.	Binding Energy (Kcal/Mol)			Compound No.	Binding Energy (Kcal/Mol)		
	CDK1 (6GU6)	CDK2 (2R3I)	CDK4 (2W9Z)		CDK1 (6GU6)	CDK2 (2R3I)	CDK4 (2W9Z)
1	-8.8	-9.2	-9.6	15	-8.2	-8.2	-8.0
2	-8.9	-8.6	-9.1	16	-8.7	-8.7	-8.8
3	-8.5	-9.4	-7.9	17	-9.6	-9.3	-9.5
4	-8.5	-9.0	-9.2	18	-7.6	-7.8	-9.4
5	-7.5	-9.1	-8.6	19	-7.8	-8.2	-8.0
6	-7.8	-8.0	-7.9	20	-8.0	-8.3	-8.1
7	-7.7	-10.1	-7.7	21	-7.6	-8.0	-8.0
8	-8.3	-9.1	-8.8	22	-7.1	-10.0	-7.2
9	-8.3	-8.8	-8.4	23	-9.9	-10.3	-10.0
10	-8.6	-8.8	-9.1	24	-8.5	-8.6	-9.1
11	-8.8	-9.0	-8.4	25	-8.2	-10.0	-9.1
12	-9.1	-9.0	-8.2	26	-7.1	-7.8	-8.0
13	-9.4	-9.5	-9.2	Palbociclib	-8.8	-8.2	-7.9
14	-8.5	-8.5	-8.4	Dinaciclib	-8.7	-8.7	-8.1

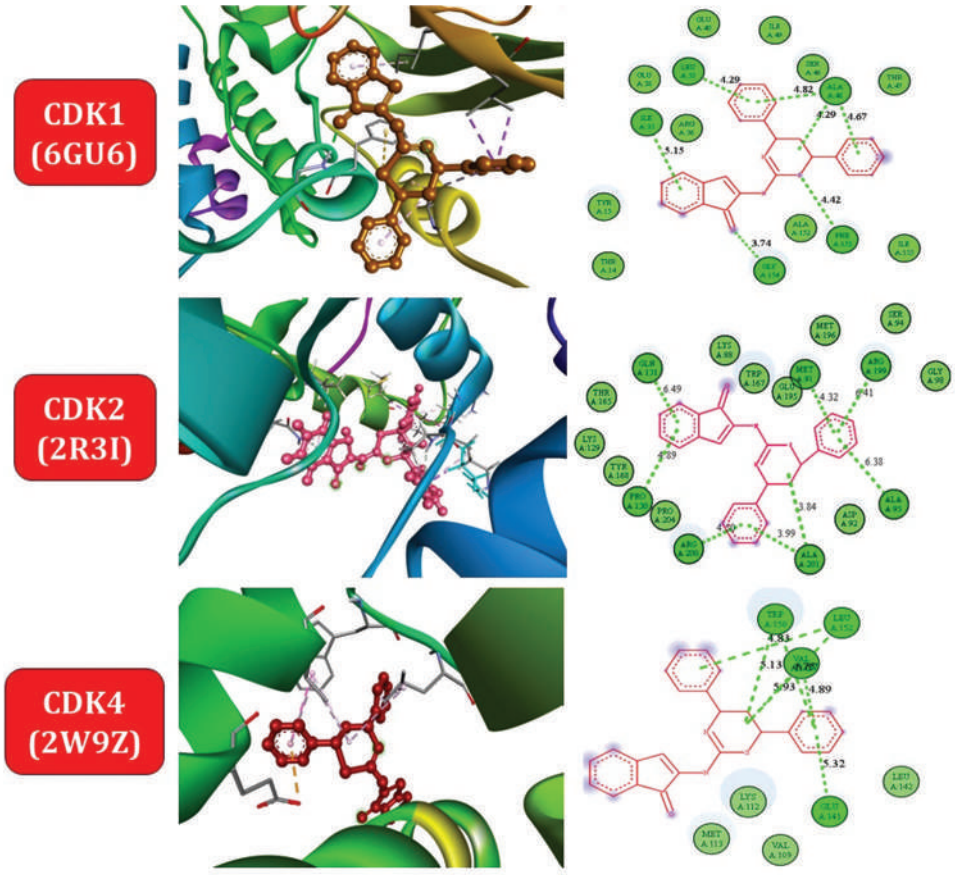

Figure 6: Docking pose and 2D Interaction Profile of compound 23 against CDKs

Table 3: Physicochemical and drug-likeness properties of the compounds using SwissADME

Compound No.	MW	HBA	HBD	NrotB	Clog P	TPSA	FCsp3	Drug likeness (Ro5)
1	523.37	5	1	6	6.05	116.03	0.12	Yes (2 violations)
2	514.53	7	1	8	5.03	134.49	0.18	Yes (1 violation)
3	540.61	5	1	8	5.03	122.51	0.23	Yes (1 violation)
4	506.53	7	1	12	3.62	175.47	0.16	Yes (0 violation)
5	495.98	5	1	11	4.56	129.65	0.16	Yes (1 violation)
6	427.53	4	0	11	6.08	47.89	0.21	Yes (1 violation)
7	426.3	4	1	4	4.2	65.79	0.14	Yes (1 violation)
8	309.4	1	0	5	5.46	12.36	0	Yes (1 violation)
9	343.85	1	0	5	5.46	12.36	0	Yes (1 violation)
10	324.42	1	1	5	5.46	38.38	0	Yes (1 violation)
11	324.42	1	1	5	5.46	38.38	0	Yes (1 violation)
12	324.42	1	1	5	5.46	38.38	0	Yes (1 violation)
13	359.46	1	0	5	6.34	12.36	0	Yes (1 violation)
14	315.45	1	0	5	5.48	12.36	0.26	Yes (1 violation)
15	248.32	1	1	4	5.48	38.38	0	Yes (1 violation)
16	291.35	2	2	6	5.48	67.48	0	Yes (1 violation)
17	414.41	5	1	8	5.48	116.03	0	Yes (1 violation)
18	401.45	5	0	8	4.65	57.12	0.12	Yes (0 violation)
19	289.71	4	3	3	4.65	73.05	0	Yes (0 violation)
20	273.26	5	3	3	4.65	73.05	0	Yes (0 violation)
21	334.16	4	3	3	4.65	73.05	0	Yes (0 violation)
22	451.9	6	1	6	3.61	84.25	0.21	Yes (0 violation)
23	396.5	3	0	3	4.79	67.09	0.26	Yes (0 violation)
24	523.34	7	1	9	3.93	118.1	0.12	Yes (1 violation)
25	557.23	5	1	8	5	72.28	0.12	Yes (1 violation)
26	368341	6	3	5	3.37	123.41	0.05	Yes (0 violation)

MW: Molecular Weight (< 500), HBA: Hydrogen bond acceptor (≤ 10); HBD: Hydrogen bond donor (≤ 5), NRB: Rotatable bonds (≤ 10), Log P: Lipophilicity (<5), TPSA: Topological polar surface area (<140), FCsp3: Fraction sp3 hybridized carbon (≥ 0.42). The limits of each parameter for druggable nature are given in parentheses

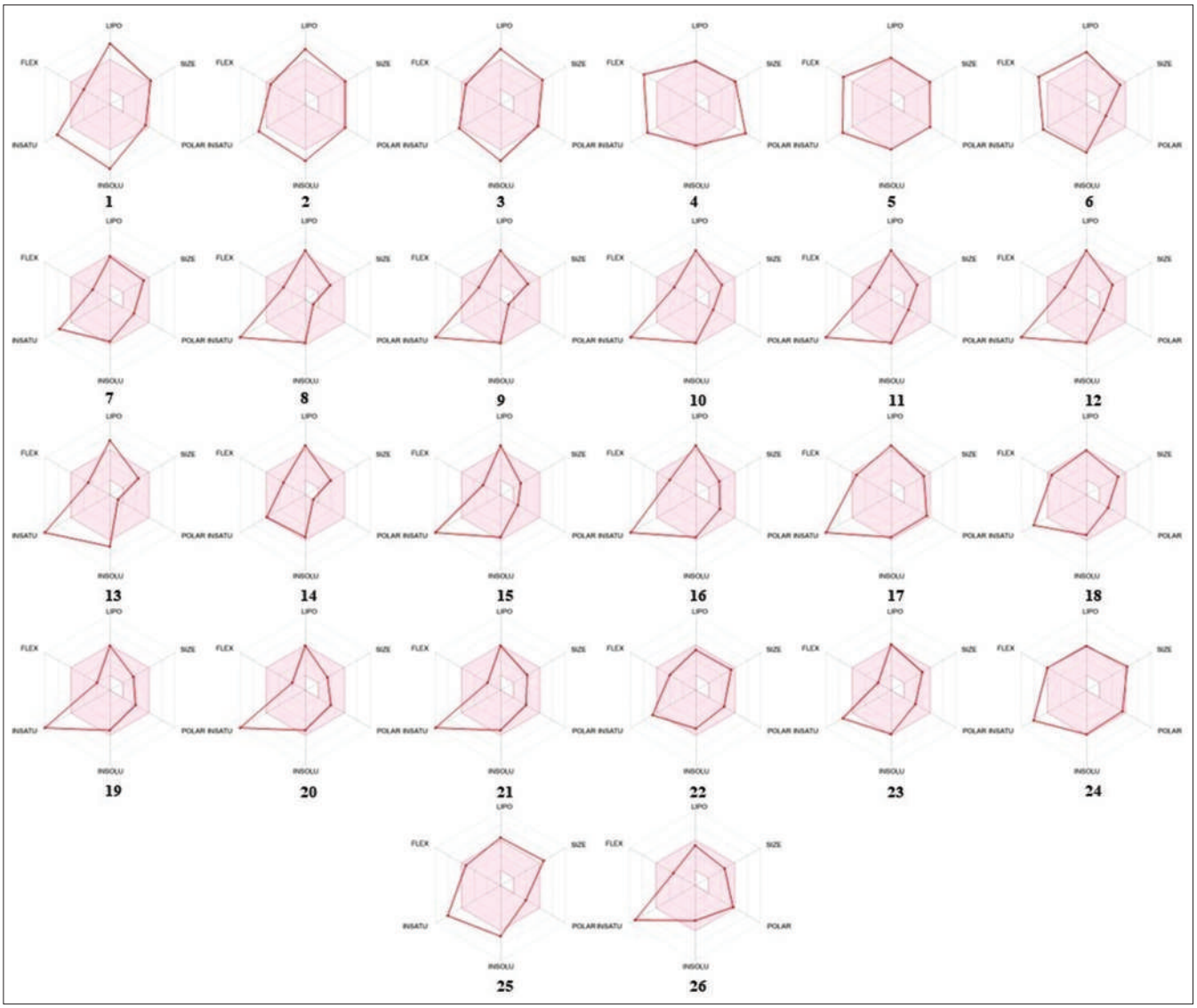

Figure 7: RADAR diagram of compounds (The coloured zone in the radar diagram is the suitable physicochemical space for oral bioavailability. LIPO (Lipophilicity): -0.7<LOG P<+5.0; SIZE: 150 g/mol<MW<500 g/mol; POLAR (Polarity): 20 Å<TPSA<130 Å; INSOLU(Insolubility): 0<LOG S<6; INSATU (Instauration): 0.25<Fraction $Csp^{3<1}$; FLEX (Flexibility): 0<Number of rotatable bonds<9)

The gastrointestinal (GI) absorption score measures the extent of absorption of a chemical from the intestine, the potent compound (compound 23) was found to be having high GI absorption, hence had excellent absorption possibility from the intestine after oral administration, while some of the compounds showed low GI absorption and hence had low absorption possibility from the intestine. Predicting the permeability of the Blood-Brain Barrier (BBB) is crucial because GI absorption and BBB permeability are deeply correlated. The blood-brain barrier (BBB) is a key biological mechanism that preserves the brain from harm. Effective medicine administration to treat illnesses of the central nervous system is also hampered by this barrier (Daina *et al.*, 2017). According to the obtained results, some of the compounds are capable of crossing the BBB and able to act on CNS. P-glycoprotein is an ATP-dependent drug efflux pump responsible for decreased drug accumulation in multidrug-resistant cells and typically causes the development of resistance to anticancer medicines. When P-gp is inhibited, a susceptible drug's bioavailability may increase and when P-gp is induced, bioavailability is decreased. Interestingly, the query molecule had the BBB permeation ability with high GI absorption, non-Pgp substrate, CYP2C19-Yes, CYP2CP-Yes, CYP3A4-Yes, CYP1A2-No and CYP2D6-No. Being the inhibition of P-gp and other results, the potent compound will have better bioavailability with better metabolism.

Human epithelial colorectal adenocarcinoma cells comprise the Caco-2 cell line. A common *in vitro* technique for the human intestinal mucosa to assess the absorption of drugs taken orally is the Caco-2 monolayer of cells. When a compound's predictive values are more than 0.9, it is said to have a high Caco-2 permeability (Morales *et al.*, 2018). In the present study, some of the compounds including the potent compound (compound 23) exhibited better Caco-2 permeability, while some possessed

less than 0.9, indicating poor permeability. When a medicine is taken orally, its principal site of absorption is typically the intestine. A substance is considered poorly absorbed if its absorption is less than 30 %. Interestingly, all the compounds were found to be having better intestinal absorption.

The theoretical volume that a drug's entire dose needs to be dispersed evenly to reach the same concentration as in blood or plasma is known as the volume of distribution (VDss). The medication delivered to tissue is greater than plasma if VD is higher. Both dehydration and renal failure may have an impact. VDss is regarded as high if it exceeds 2.81 L/kg (log VDss > 0.45) and low if it is less than 0.71 L/kg (log VDss < -0.15) (Pires *et al.*, 2018). In animal models, blood-brain barrier permeability is quantified *in vivo* as log BB, or the logarithmic ratio of drug concentrations in the brain to plasma. For a particular substance, a logBB value larger than 0.3 is believed to quickly penetrate the blood-brain barrier, while molecules with logBB value less than -1 are poorly dispersed to the brain (Raju *et al.*, 2023).

The body's major detoxifying enzyme, cytochrome P450, is mostly located in the liver. It aids in the xenobiotic's excretion by metabolizing them. The cytochrome P450s can both activate and deactivate a variety of medicines. Substrates or inhibitors of this enzyme should not be used together since they may alter how drugs are metabolized. Therefore, it›s critical to evaluate a compound›s potential to function as a substrate as well as its capacity to block this enzyme›s many isoforms. Our findings revealed that some of the compounds are substrates and some are inhibitors. The potent compound was found to be both substrate and inhibitor of CYP3A4 and non-inhibitor and non-substate of CYP2D6 isoforms.

The constant of proportionality Drug clearance is computed using CL_{tot} and is essentially the sum of renal and hepatic clearance (liver metabolism and biliary clearance). In order to achieve steady-state concentrations, it is crucial to ascertain the dosage rates, which are closely linked to bioavailability. The compound's projected total clearance is expressed in log (mL/min/kg). Renal Organic Cation Transporter 2 (OCT2) is a renal uptake transporter that plays an important role in the distribution and renal clearance of pharmaceuticals and endogenous chemicals. When OCT2 inhibitors are also provided together, there may be unfavourable interactions between the two drugs. Evaluating a molecule's ability to be transported by OCT2 yields important details about its clearance as well as any possible contraindications (Pires *et al.*, 2018). Hence, the results revealed that none of the compounds are the substrates of renal OCT2. The pharmacokinetic properties of the tested compounds are given in Table 4.

One of the most important steps in the drug development process is the prediction of chemical toxicity. In addition to being quicker than estimating lethal concentrations in animals, computational toxicity estimations may also lessen the number of animal tests conducted. Drug displacement is largely caused by drug-induced liver injury, which is a serious safety risk for drug development. A substance was classified as

Table 4: Pharmacokinetic properties of the compounds using SwissADME and pkCSM

Compound No.	GI Absorption	BBB Permeant	ABSORPTION		DISTRIBUTION			METABOLISM				EXCRETION	
			CaCo2 Permeability	HIA (%)	VD_{ss}	BBB Permeability	Fraction Unbound	CYP2D6 Substrate	CYP3A4 Substrate	CYP2D6 Inhibitor	CYP3A4 Inhibitor	Total Clearance	Renal OCT2 Substrate
1	Low	No	0.293	100	-0.536	-1.01	0	No	Yes	No	No	-0.312	No
2	Low	No	0.233	100	-0.766	-1.13	0	No	Yes	No	Yes	0.054	No
3	Low	No	0.339	100	-0.572	-0.973	0	No	Yes	No	No	0.443	No
4	Low	No	-0.372	94.742	-0.369	-1.222	0.014	No	Yes	No	Yes	0.204	No
5	Low	No	0.965	100	-0.438	-0.914	0	No	Yes	No	Yes	0.168	No
6	High	No	1.074	93.243	0.298	-0.095	0	No	Yes	No	Yes	0.259	No
7	High	Yes	0.669	92.455	0.229	0.063	0.095	No	Yes	No	Yes	-0.092	No
8	Low	No	1.591	93.997	0.475	0.664	0	No	Yes	No	No	0.616	No
9	Low	No	1.339	92.836	0.169	0.847	0	Yes	Yes	Yes	No	0.077	No
10	Low	No	1.076	91.265	0.597	-0.021	0	No	Yes	No	No	0.356	No
11	Low	No	1.314	91.84	0.062	0.25	0	No	Yes	Yes	No	0.398	No
12	Low	No	1.314	91.84	0.062	0.25	0	No	Yes	Yes	No	0.391	No
13	Low	No	1.367	93.729	0.08	0.916	0	Yes	Yes	Yes	No	0.648	No
14	Low	No	1.703	94.458	1.138	0.664	0	No	Yes	No	No	0.246	No
15	Low	No	1.501	92.173	0.602	0.143	0	No	Yes	No	No	0.304	No
16	Low	No	0.854	89.457	0.209	-0.192	0	No	Yes	No	No	0.657	No
17	Low	No	0.288	99.657	-0.507	-0.752	0	No	Yes	No	Yes	0.142	No
18	High	Yes	1.077	96.541	-0.201	-0.115	0.016	No	Yes	No	Yes	0.17	No
19	High	Yes	0.977	90.38	-0.136	-1.002	0.145	No	No	No	Yes	0.01	No
20	High	Yes	1.057	90.577	-0.093	-0.823	0.197	No	No	No	No	0.149	No
21	High	Yes	0.972	90.313	-0.125	-1.023	0.142	No	No	No	Yes	-0.011	No
22	High	No	1.108	95.612	0.245	-0.914	0.102	No	Yes	No	Yes	0.214	No
23	High	Yes	1.092	93.654	0.451	0.321	0	No	Yes	No	Yes	0.165	No
24	High	No	0.702	95.464	-0.291	-1.123	0	No	Yes	No	Yes	-0.225	No
25	High	No	1.247	89.772	-0.034	-0.776	0	No	Yes	No	Yes	-0.282	No
26	High	No	0.723	84.333	0.107	-1.191	0.048	No	Yes	No	Yes	0.235	No

Caco2 (Human epithelial colorectal adenocarcinoma cells) Permeability, PGP-P-Glycoprotein, HIA-Human Intestinal Absorption, VD_{ss} - Volume of Distribution, BBB-Blood brain barrier, CYP-Cytochrome P450 enzymes, Renal Organic Cation Transporter

hepatotoxic if it caused at least one physiological or pathological liver event that was closely linked to the liver's normal function being interrupted. The ability of a chemical to cause cancer, raise the risk of cancer or accelerate the progression of cancer is known as carcinogenicity. The ability of a substance to alter genetic information is known as mutagenicity. Many chemicals disrupt DNA with prolonged exposure, which can result in cell death or mutation. Cytotoxicity is the property of being toxic to living cells. Hence the prediction of these organ toxicities is crucial for developing a better drug molecule. Our investigation showed that the majority of the compounds are non-hepatotoxic, 50% of the compounds are carcinogenic, immunotoxic and mutagenic in nature. Interestingly, none of the compounds are cytotoxic, indicating that all the compounds are safe in normal healthier cell lines. Along with the LD_{50} and toxicity classes of the compounds were also predicted. The LD_{50} is the amount of a drug that, when administered all at once, causes 50% death in a group of test animals. The results showed that all the compounds belong to the toxicity class 4 and 5 where the predicted LD_{50} was between 300-5000 mg/kg except compound 22 with high toxicity (class 3) and 6 with highly safe (class 6), indicating that all of the tested compounds are safe with lesser toxicity. The predicted toxicity classes, LD_{50} values and organ toxicities are given in Table 5.

Because of their poisonous properties, most tiny organic compounds were unable to be transformed into therapeutic components. Using the CardiotoxCSM Webserver, the cardiac toxicity profile of the selected compounds was determined. This tool yielded information on arrhythmia, heart block, cardiac failure, hERG toxicity, hypertension and myocardial infarction, which is shown in Table 6. Inhibition of the Potassium channels encoded by hERG is the major mechanism for the development of acquired long QT Syndrome leading to catastrophic ventricular arrhythmia. Numerous drugs have been taken off from the pharmaceutical market due to hERG channel inhibition. A given compound's likelihood of being a hERG inhibitor will be ascertained by the predictor. The potent compound (23) was found to be safe, with non-risk factors of cardiotoxicity including arrhythmia, cardiac failure, heart block, hERG toxicity and hypertension except myocardial infarction. Some of the compounds exhibited cardiotoxicity by having risk factors on the above shown conditions.

Theoretical Studies

FMO and MEP analysis

The optimized molecular structure (Figure 8a) of the potent compound (compound 23) was derived using Gaussian 09 W and GaussView 6.0 software. The structural parameters of the optimized structure were obtained using DFT (B3LYP) using the 6-31 G ++ (d, p) basis set. The primary orbitals involved in chemical reactions are the Frontier molecular orbital, Highest Occupied Molecular Orbital (HOMO), which represents the electron acceptor distribution, and Lowest Unoccupied Molecular Orbital (LUMO), which represents the electron donor distribution. The energy gap, which measures the difference between a molecule's HOMO and LUMO, is used to assess a molecule's molecular electron transport capacity and chemical stability. Descriptors such as chemical reactivity, chemical hardness, chemical softness, electronegativity, kinetic

Table 5: Toxicity prediction of compounds using protox II webserver

Compound ID	Predicted LD50 (mg/kg)	Predicted Toxicity Class	Hepatotoxicity	Carcinogenicity	Immunotoxicity	Mutagenicity	Cytotoxicity
1	3000	5	Inactive	Inactive	Active	Inactive	Inactive
2	3000	5	Inactive	Inactive	Active	Inactive	Inactive
3	3000	5	Inactive	Active	Active	Active	Inactive
4	507	4	Inactive	Active	Inactive	Active	Inactive
5	4000	5	Inactive	Active	Inactive	Active	Inactive
6	2100	5	Inactive	Inactive	Active	Active	Inactive
7	1000	4	Inactive	Inactive	Inactive	Inactive	Inactive
8	430	4	Inactive	Inactive	Inactive	Active	Inactive
9	430	4	Inactive	Active	Inactive	Active	Inactive
10	430	4	Inactive	Active	Inactive	Active	Inactive
11	430	4	Inactive	Active	Inactive	Active	Inactive
12	430	4	Inactive	Active	Inactive	Active	Inactive
13	430	4	Inactive	Inactive	Inactive	Active	Inactive
14	3000	5	Inactive	Inactive	Inactive	Active	Inactive
15	2560	5	Active	Active	Inactive	Active	Inactive
16	817	4	Active	Active	Inactive	Inactive	Inactive
17	2690	5	Active	Active	Active	Active	Inactive
18	2100	5	Active	Active	Active	Inactive	Inactive
19	1800	4	Inactive	Inactive	Active	Inactive	Inactive
20	2000	4	Inactive	Inactive	Active	Inactive	Inactive
21	1000	4	Inactive	Inactive	Active	Inactive	Inactive
22	6000	6	Active	Inactive	Active	Inactive	Inactive
23	430	4	Active	Inactive	Inactive	Inactive	Inactive
24	536	4	Active	Active	Active	Active	Inactive
25	500	4	Active	Active	Inactive	Active	Inactive
26	388	3	Active	Inactive	Active	Inactive	Inactive

LD50: Lethal dose (mg/kg), Class 1: Fatal if swallowed (LD50≤5), Class 2: Fatal if swallowed (5 < LD50 ≤ 50), Class 3: Toxic if swallowed (50 < LD50 ≤ 300), Class 4: Harmful if swallowed (300 < LD50≤2000), Class 5: May be harmful if swallowed (2000 < LD50≤5000)

Table 6: Cardiotoxicity of the compounds by using Cardio ToxCSM

Compound No.	Arrhythmia	Cardiac Failure	Heart Block	hERG-Toxicity	Hypertension	Myocardial Infarction
1.	0	0	0	0	1	1
2.	0	0	0	0	1	0
3.	1	0	0	1	1	0
4.	0	0	0	1	0	0
5.	0	0	0	1	0	1
6.	0	0	0	1	1	1
7.	0	0	0	0	1	1
8.	0	0	0	0	0	1
9.	0	1	0	0	0	1
10.	0	0	0	0	0	0
11.	0	0	0	0	0	0
12.	0	1	0	0	0	0
13.	0	0	0	0	0	0
14.	0	0	0	1	0	1
15.	0	0	0	0	0	0
16.	0	0	0	0	0	0
17.	0	0	0	0	0	0
18.	0	0	0	1	1	1
19.	0	0	0	0	1	0
20.	0	0	0	0	0	0
21.	0	0	0	0	0	0
22.	0	0	0	1	1	1
23.	0	0	0	0	0	1
24.	0	0	0	0	0	1
25.	0	0	0	0	0	0
26.	0	0	0	0	0	1

hERG - Human ether-a-go-go gene

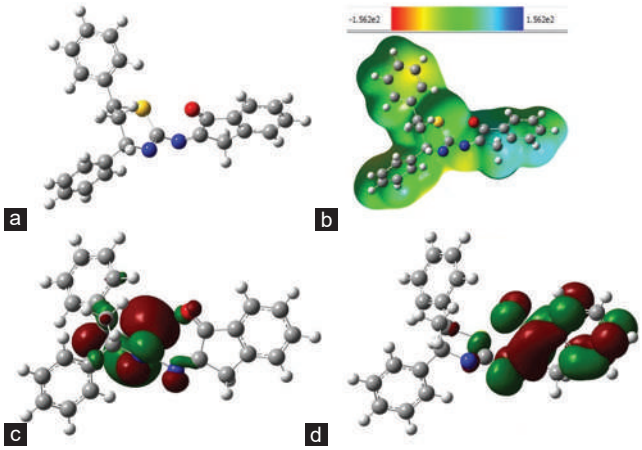

Figure 8: a) Optimized Structurea, b) Electron Density Map, c) LUMO, d) HOMO of Compound 23

stability and aromaticity can be computed using the acquired energy gap. The filled π-orbitals (HOMO) are seen mostly in the thiazin-2-yl-imino linkage portion and the unfilled anti-π-orbital (LUMO) are seen in the dihydro-1H-inden-1-one part, respectively. From these results, it was shown that the electron transitions take place from the thiazin-2-yl-imino linkage portion to the dihydro-1H-inden-1-one part i.e., HOMO to LUMO, respectively (Figures 8b & 8c).

The molecular electrostatic potential (MEP), a helpful descriptor for identifying the interactions between molecules and their electrophilic and nucleophilic character, is connected to the electron density. Additionally, it displays the charge distributions together with particular indications of the compound interactions. DFT/B3LYP was used to compute the compound's MEP-mapped surface (Figure 8d) at the 6-31 G ++ (d, p) basis set. The red area in a MEP represents the high electronegativity portion; the blue region represents the electrostatic region with a partial positive charge (electropositive); the yellow region represents the slightly electron-rich region and the green region represents the zero potential (neutral).

Global Reactivity Descriptors

The global descriptors, such as electrophilicity index (ω), softness (S), hardness (∫), electronegativity (χ) and chemical potential (μ) are developed and computed utilizing the obtained E HOMO and E LUMO. These characteristics are crucial for assessing the compound's stability. The hardness and softness of two types of molecules such as hard and soft are determined by their respective HOMO-LUMO energy gap values. Hard molecules have larger energy gap values than soft molecules. This allows for the measurement of both types of molecule's stability and reactivity. The electronic transfer occurring within the molecule is affected by the energy gap. Less energy gap in the molecules makes electronic transfer easier. The biological activity of the compound was related to the stability of the compound, hardness and by means of energy gap values (Hassan *et al.*, 2023). By this way, compound 23 was found to possessing better hardness values as shown above and correlated with the biological potential, determined by the molecular docking studies. The calculated values of the global reactivity descriptors are given in Table 7.

Table 7: Quantum chemical descriptors of the Compound 23

Parameters	Compound
HOMO (eV)	-0.2190
LUMO (eV)	-0.0944
Energy gap (eV)	0.1246
Ionization potential	0.2190
Electron affinity	0.0944
Electronegativity	0.1567
Chemical potential	-0.1567
Chemical hardness	0.0623
Chemical softness	1.7578
Electrophilicity index	0.1971

eV: Energy Gap, [I= -EHOMO] (eV): Ionization potential, [A= -ELUMO] (eV): Electron affinity, [χ= (I+A)/2]: Electronegativity, [μ= - χ]: Chemical potential, [η= (I - A)/2]: Chemical hardness, [S=I/2η]: Chemical softness, [ω= μ^2/2 η]: Electrophilicity index

CONCLUSION

Cancer is the most common cause of death worldwide. Various signalling pathways are associated with the development of cancer. Among those pathways, the Cyclin-dependent kinase pathway plays a major role in the development of cancer cells. Targeting the CDK signalling pathway with different Chalcone-Schiff base hybrids might be a promising option. Based on the network pharmacology approach, various isoforms of CDKs are identified as the most prominent targets for the synthesized compounds. These 26 different Chalcone-Schiff base hybrids along with standard drugs were evaluated for anti-CDK activity using molecular docking studies and the results revealed that all the screened compounds exhibit different levels of inhibitory potential against CDK isoforms. Among them, the compound 23 ((Z)-2-((4,6-diphenyl-5,6-dihydro-4H-1,3-thiazin-2-yl)imino)-2,3-dihydro-1H-inden-1-one) was identified as most potent compound than the tested standards against the CDK isoforms with better binding energy and interaction profile. The most active compound, ((Z)-2-((4,6-diphenyl-5,6-dihydro-4H-1,3-thiazin-2-yl)imino)-2,3-dihydro-1H-inden-1-one) was also screened for various physicochemical, pharmacokinetic and toxicity properties, the results indicated that this compound was druggable with the better pharmacokinetic and metabolic profile. Along with these properties, the theoretical studies were performed at the DFT level and the better stability and bioactivity in the biological system of the compound were proved. Therefore, these Chalcone-Schiff base hybrids can be used for the effective treatment of cancer by targeting CDKs and further *in vitro* and *in vivo* biological studies are required to confirm the potency of these compounds.

ACKNOWLEDGEMENT

We thank the Management and Dr. G. Murugananthan, Principal of our college for giving constant support and encouragement for writing this research article.

REFERENCES

Abdullah, J. A., Aldahham, B. J. M., Rabeea, M. A., Asmary, F. A., Alhajri, H. M., & Islam, M. A. (2021). Synthesis, Characterization and In-Silico Assessment of Novel Thiazolidinone Derivatives for Cyclin-Dependent Kinases-2 Inhibitors. *Journal of Molecular Structure, 1223*, 129311. https://doi.org/10.1016/j.molstruc.2020.129311

Ahmed, A. A., Mahmood, I, Q., & Aziz, H. S. (2022). Synthesis and Characterization of Few New Substituted 1, 3, 4-Oxadiazoles 1, 2, 4-Triazoles and Schiff Bases via Chalcone Compounds. *International Journal of Drug Delivery Technology, 12*(3), 1087-1092. https://doi.org/10.25258/ijddt.12.3.27

Aiwonegbe, A. E., & Usifoh, C. O. (2021). Synthesis, Infra Red Characterization and Antimicrobial Evaluation of Schiff bases Derived from 1, 3-Diphenylprop-2-en-1-one and 1-Phenyl-3-(4-Chlorophenyl)-prop-2-en-1-one. *Journal of Chemical Society of Nigeria, 46*(2), 197-204. https://doi.org/10.46602/jcsn.v46i2.596

Ajani, O. O., Jolayemi, E. G., Owolabi, F. E., Tolubolaji, O. O., & Audu, O. Y. (2021). Heterogeneous acid Catalyzed Synthesis and Spectroscopic Characterization of Schiff bases Derived from Chalcone Derivatives. *Egyptian Journal of Chemistry, 64*(1), 193-200. https://doi.org/10.21608/ejchem.2020.20610.2233

Badal, M. M. R., Hossain, M. Z., Maniruzzaman, M., & Yousuf, M. A. (2020). Synthesis, Identification and Computational Studies of Novel Schiff bases N-(2, 6-Dibenzylidenecyclohexylidene)-N"-(2, 4-Dinitrophenyl) Hydrazine Derivatives. *SN Applied Sciences, 2*, 1914. https://doi.org/10.1007/s42452-020-03745-4

Chen, X., Robinson, D. G., & Storey, J. D. (2021). The Functional False Discovery Rate with Applications to Genomics. *Biostatistics, 22*(1), 68-81. https://doi.org/10.1093/biostatistics/kxz010

Daina, A., Michielin, O., & Zoete, V. (2017). SwissADME: a free web tool to evaluate pharmacokinetics, drug-likeness and medicinal chemistry friendliness of small molecules. *Scientific Reports, 7*, 42717. https://doi.org/10.1038/srep42717

Dangwal, K. L., & Semwal, A. R. (2016). Microwave Assisted Synthesis and Characterization of Oxime Derivatives of Substituted Chalcones. *International Journal of Science and Research, 5*(7), 356-358.

Datar, M., Dhanwad, R., Javeed, M., Yernale, N. G. & Mathada, B. S. (2024). Synthesis, Structural Investigations, DFT Calculations, and Molecular Docking Studies of Novel 2-(Substituted-Aryloxymethyl)-5-(Pyridin-4-yl)-1, 3, 4-Oxadiazoles: Highly potential InhA and Cytochrome c Peroxidase Inhibitors. *Polycyclic Aromatic Compounds, 44*(1), 473-487. https://doi.org/10.1080/10406638.2023.2174997

Ejaz, S. A., Saeed, A., Siddique, M. N., un Nisa, Z., Khan, S., Lecka, J., Sévigny, J., & Iqbal, J. (2017). Synthesis, Characterization and Biological Evaluation of Novel Chalcone Sulfonamide Hybrids as Potent Intestinal Alkaline Phosphatase Inhibitors. *Bioorganic Chemistry, 70*, 229-236. https://doi.org/10.1016/j.bioorg.2017.01.003

Ermiş, E. (2018). Synthesis, Spectroscopic Characterization and DFT Calculations of Novel Schiff base Containing Thiophene Ring. *Journal of Molecular Structure, 1156*, 91-104. https://doi.org/10.1016/j.molstruc.2017.11.089

Fandaklı, S., Doğan, İ. S., Sellitepe, H. E., Yaşar, A., & Yaylı, N. (2018). Synthesis, Theoretical Calculation and α-Glucosidase Inhibition of New Chalcone Oximes. *Organic Communications, 11*(1), 23-24. http://doi.org/10.25135/acg.oc.38.18.02.067

Ghafouri-Fard, S., Khoshbakht, T., Hussen, B. M., Dong, P., Gassler, N., Taheri, M., Baniahmad, A., & Dilmaghani, N. A. (2022). A eview on the Role of Cyclin Dependent Kinases in Cancers. *Cancer Cell International, 22*, 325. https://doi.org/10.1186/s12935-022-02747-z

Hassan, A. S., Morsy, N. M., Aboulthana, W. M., & Ragab, A. (2023). Exploring Novel Derivatives of Isatin-based Schiff bases as Multi-target Agents: Design, Synthesis, in Vitro Biological Evaluation, and in Silico ADMET Analysis with Molecular Modeling Simulations. *RSC Advances, 13*, 9281-9303. https://doi.org/10.1039/D3RA00297G

Ibrahim, T. S., Almalki, A. J., Moustafa, A. H., Allam, R. M., Abuo-Rahma, G. E. D. A., El Subbagh, H. I., & Mohamed, M. F. A. (2021). Novel 1, 2, 4-Oxadiazole-Chalcone/Oxime Hybrids as Potential Antibacterial DNA Gyrase Inhibitors: Design, Synthesis, ADMET Prediction and Molecular Docking Study. *Bioorganic Chemistry, 111*, 104885. https://doi.org/10.1016/j.bioorg.2021.104885

Izadi, S., Hojjat-Farsangi, M., Karpisheh, V., & Jadidi-Niaragh, F. (2023). Pan Cyclin-Dependent Kinase Inhibitors for the Treatment of Breast Cancer. *International Journal of Drug Research in Clinics, 1*, e2. https://doi.org/10.34172/ijdrc.2023.e2

Jamel, N. M., Hussein, D. F., & Tomma, J. H. (2017). Synthesis and Characterization New Schiff Bases, Pyrazole and Pyrazoline Compounds Derived From Acid Hydrazide Containing Isoxazoline Ring. *Ibn AL-Haitham Journal for Pure and Applied Science*, *27*(3), 435-447.

Kawsar, M., Taz, T. A., Paul, B. K., Mahmud, S., Islam, M. M., Bhuyian, T., & Ahmed, K. (2020). Analysis of Gene Network Model of Thyroid Disorder and Associated Diseases: A bioinformatics Approach. *Informatics in Medicine Unlocked, 20*, 100381. https://doi.org/10.1016/j.imu.2020.100381

Kombo, D. C., Tallapragada, K., Jain, R., Chewning, J., Mazurov, A. A., Speake, J. D., Hauser, T. A., & Toler, S. (2013). 3D Molecular Descriptors Important for Clinical Success. *Journal of Chemical Information and Modeling, 53*(2), 327-342. https://doi.org/10.1021/ci300445e

Li, S., Shao, Y., Chen, H., & Wang, J. (2022). Using Network Pharmacology to Systematically Decipher the Potential Mechanisms of Jisuikang in the Treatment of Spinal cord Injury. *Evidence-Based Complementary and Alternative Medicine, 2022*, 4932153. https://doi.org/10.1155/2022/4932153

Liu, J., Liu, J., Tong, X., Peng, W., Wei, S., Sun, T., Wang, Y., Zhang, B., & Li, W. (2021). Network Pharmacology Prediction and Molecular Docking-based Strategy to Discover the Potential Pharmacological Mechanism of Huai Hua San against Ulcerative Colitis. *Drug Design, Development and Therapy, 15*, 3255-3276. https://doi.org/10.2147/DDDT.S319786

Liu, Y.-T., Sheng, J., Yin, D.-W., Xin, H., Yang, X.-M., Qiao, Q.-Y., & Yang, Z. J. (2018). Ferrocenyl Chalcone-based Schiff bases and their Metal Complexes: Highly Efficient, Solvent-free Synthesis, Characterization, Biological Research. *Journal of Organometallic Chemistry, 856*, 27-33. https://doi.org/10.1016/j.jorganchem.2017.12.022

Luo, Y., Song, R., Li, Y., Zhang, S., Liu, Z.-J., Fu, J., & Zhu, H.-L. (2012). Design, Synthesis, and Biological Evaluation of halcone Oxime Derivatives as Potential Immunosuppressive Agents. *Bioorganic & Medicinal Chemistry Letters, 22*(9), 3039-3043. https://doi.org/10.1016/j.bmcl.2012.03.080

Morales, A. M., Mukai, R., Murota, K., & Terao, J. (2018). Inhibitory Effect of Catecholic Colonic Metabolites of Rutin on Fatty acid Hydroperoxide and Hemoglobin Dependent Lipid Peroxidation in Caco-2 Cells. *Journal of Clinical Biochemistry and Nutrition, 63*(3), 175-180. https://doi.org/10.3164/jcbn.18-38

Morris, G. M., Huey, R., Lindstrom, W., Sanner, M. F., Belew, R. K., Goodsell, D. S., & Olson, A. J. (2009). AutoDock4 and AutoDockTools4: Automated Docking with Selective Receptor Flexibility. *Journal of Computational Chemistry, 30*(16), 2785-2791. https://doi.org/10.1002/jcc.21256

Muleta, F., & Desalegn, T. (2022). Synthesis, In Silico, and Biological Applications of Novel Heteroleptic Copper (II) Complex of Natural Product-Based Semicarbazone Ligands. *Journal of Chemistry, 2022*, 1497117. https://doi.org/10.1155/2022/1497117

Pacey, S., Sarker, D., & Workman, P. (2008). Pharmacokinetics and pharmacodynamics in drug development. In M. Schwab (Eds.), *The Encyclopedia of Cancer* (pp. 2306-2309). Berlin, Germany: Springer.

Pires, D. E. V., Kaminskas, L. M., & Ascher, D. B. (2018). Prediction and Optimization of Pharmacokinetic and Toxicity Properties of the Ligand. In M. Gore, U. B. Jagtap (Eds.), *Computational Drug Discovery and Design* (pp. 271-284) Berlin, Germany: Springer. https://doi.org/10.1007/978-1-4939-7756-7_14

Radhakrishnan, S. K., Shimmon, R. G., Conn, C., & Baker, A. T. (2016). Evaluation of Novel Chalcone Oximes as Inhibitors of Tyrosinase and Melanin Formation in B16 Cells. *Archiv der Pharmazie, 349*(1), 20-29. https://doi.org/10.1002/ardp.201500298

Raju, S. K., Kumar, S., Sekar, P., Sundhararajan, N., & Nagalingam, Y. (2023). Ligand Based Multi-Targeted Molecular Docking Analysis of Terpenoid Phytoconstituents as Potential Chemotherapeutic Agents Against Breast Cancer: An In Silico Approach. *Journal of Pharmaceutical Research, 22*(2), 55-62. https://doi.org/10.18579/jopcr/v22.2.23.5

Riazimontazer, E., Sadeghpour, H., Nadri, H., Sakhteman, A., Küçükkılınç, T. T., Miri, R., & Edraki, N. (2019). Design, Synthesis and Biological Activity of Novel Tacrine-Isatin Schiff base Hybrid Derivatives. *Bioorganic Chemistry, 89*, 103006. https://doi.org/10.1016/j.bioorg.2019.103006

Rohini, C., Arasan, K. T., Jagadeeshbabu, V., & Saritha, M. (2021). Synthesis and IR Spectroscopic Characterization of some synthesized Chalcone linked Isatin Derivatives -Based Schiff Bases. *International Journal of Current Research, 13*(10), 19355-19357.

Sekar, P., Kumar, S., & Raju, S. K. (2023a). An Updated Review on Recent Advancements in the Diverse Biological Applications of Medicinally Privileged Scaffold: Chalcone and its Derivatives. *International Journal of Medical Sciences and Pharma Research, 9*(1), 7-20. https://doi.org/10.22270/ijmspr.v9i1.61

Sekar, P., Kumar, S., & Raju, S. K. (2023b). A Review on Chemistry, Synthesis and Biological Applications of Chalcone-based Schiff Bases. *Journal of Drug Delivery and Therapeutics, 13*(3), 145-154. https://doi.org/10.22270/jddt.v13i3.5969

Shannon, P., Markiel, A., Ozier, O., Baliga, N. S., Wang, J. T., Ramage, D., Amin, N., Schwikowski, B., & Ideker, T. (2003). Cytoscape: A Software Environment for Integrated Models of Biomolecular Interaction Networks. *Genome Research, 13*, 2498-2504. https://doi.org/10.1101/gr.1239303

Shawky, E. (2019). Prediction of Potential Cancer-related Molecular Targets of North African Plants Constituents using Network Pharmacology-based Analysis. *Journal of Ethnopharmacology, 238*, 111826. https://doi.org/10.1016/j.jep.2019.111826

Siddiqui, E. J., Azad, I., Khan, A. R., & Khan, T. (2019). Thiosemicarbazone Complexes as Versatile Medicinal Chemistry Agents: a Review. *Journal of Drug Delivery and Therapeutics, 9*(3), 689-703.

Soman, S. S., & Jain, P. (2022). Design, Synthesis and Study of Calamitic Liquid Crystals containing Chalcone and Schiff Base Linkages along with Terminal Alkoxy Chain. *Journal of Advanced Scientific Research, 13*(4), 59-68. https://doi.org/10.55218/JASR.202213411

Susanti, N. M. P., & Tjahjono, D. H. (2021). Cyclin-dependent Kinase 4 and 6 Inhibitors in Cell Cycle Dysregulation for Breast Cancer Treatment. *Molecules, 26*(15), 4462. https://doi.org/10.3390/molecules26154462

Thakare, A. P., & Mandlik, P. R. (2017). Co(II), Ni(II), Cu(II) And Cr(III) Complexes Of Heterocyclic Schiff Base Ligand: Synthesis, Spectroscopic And Thermal Study. *International Journal of Advanced Research and Publications, 1*(2), 1-5.

Thakare, A. P., & Mandlik, P. R. (2021). Synthesis, Spectroscopic and Thermal Studies of Fe(III) and VO(IV) Complexes of Heterocyclic Schiff Base Ligand. *Indian Journal of Advances in Chemical Science, 5*(4), 318-323.

Vadivelu, A., Saranya, A., & Gopal, V. (2014). Molecular Docking, Synthesis and Biological Evaluation of New Schiff Bases of 2, 3 Disubstituted Quinazolinone Derivatives. *International Journal of Pharmacy & Therapeutics, 5*(2), 90-99.

Vyas, S. P. (2018). Synthesis and Characterization of New Schiff-Base Derived from (2Z)-1-(2, 4-Dimethylphenyl)-3-(4-Hydroxy-3-Methoxyphenyl) Prop-2-En-1-One. *Journal of Chemical and Pharmaceutical Research, 10*(1), 200-202.

Vyas, S. P., Daraji, K. M., Darji, P., Patel, P. A., Goswami, T. K., & Goswami, K. V. (2016). Preparation and Characterizations of (2e)-1-(4-{(E)- [(3,4,5- Trimethoxy Phenyl) Methylidene]Amino} Phenyl)- 3-Phenylprop-2-En-1-One. *World Journal of Pharmaceutical Research, 5*(5), 928-31.

View publication stats